Journal of Peptide Science, Vol. 3, 65–81 (1997)

Lipid-induced Secondary Structures and Orientations of [Leu^5]-enkephalin: Helical and Crystallographic Double-bend Conformers Revealed by IRATR and Molecular Modelling

ROBERT SCHWYZER, PANAGIOTA MOUTEVELIS-MINAKAKIS, SHUNSAKU KIMURA and HANS-ULRICH GREMLICH

Institute of Molecular Biology and Biophysics, Swiss Federal Institute of Technology (ETH), Zürich, Switzerland

Received 14 May 1996
Accepted 10 June 1996

Abstract: Lipid-induced secondary structures and orientations of the two enantiomeric [Leu^5]-enkephalins, L-Tyr-Gly-Gly-L-Phe-L-Leu, and D-Tyr-Gly-Gly-D-Phe-D-Leu, on flat multi-bilayers of 1-palmitoyl-2-oleoyl-*sn*-glycero-3-phosphocholine (POPC) were examined with polarized attenuated total reflection IR (IRATR) spectroscopy and molecular mechanics procedures. The membrane-bound peptides showed identical IR spectra in the amide I and II band regions that indicated membrane-induced secondary structures and specific orientations of the non-zwitterionic molecules. A Lorentzian band shape analysis based on second derivatives of the original curves and the observed band polarizations suggested the presence of helical structures (β_{III}-and α-turns), oriented more or less perpendicular to the membrane surface. Other folded structures, *e.g.* β_I- and γ turns, were not excluded. Molecular modelling of non-zwitterionic [Leu^5]-enkephalin with two β_{III}-turns or an α-turn resulted in essentially four low-energy conformers containing (i) two β_{III}-turns, (ii) one α-turn, (iii) a β_{III}-turn fused to an α-turn, and (iv) a β_{III}-turn fused to a β_I-turn as in the crystallographic molecular conformation described by Aubry *et al.* [*Biopolymers* **28**, 27–40 (1989)]. Zwitterionic [Leu^5]-enkephalin with two β_{III}-turns collapsed to a C_{13} turn (a distorted α-turn) bridged by a γ_I-turn (v). The alignment of the amide I oscillators within the helical structures, (i), (ii) and (iii), and the double-bend structures, (iv) and (v), explained the observed amide I and II polarizations. Differences between these and other lipid-induced [Leu^5]-enkephalin conformers reported in the literature may be caused by the lipid polymorphism of the model membranes used. Possible implications of the new conformers for the molecular mechanism of opioid receptor selection are discussed in terms of the membrane compartments theory.

Keywords: [Leu^5]-enkephalin; secondary structure; IRATR; MMX force field; bioactive conformation

INTRODUCTION

The endogenous opioid peptide, leucine enkephalin [1], elicits antinociceptive, cardiovascular and immune-regulatory responses through stereospecific, selective interactions with three main types of opioid receptor: δ, μ and κ (the affinities decrease in this order [2, 3]). In 1982, Schiller and DiMaio [4] published pharmacological and chemical evidence obtained from cyclic enkephalin analogues suggesting that the opioid receptor subclasses, particularly δ and μ, require different 'bio-active' conformations of the bound enkephalin molecules for stimulation. This view was supported by further work (e.g. [5, 6]) and the question arose as to whether or not such bioactive conformations were identical with single, preferred conformations of endogenous enkephalins in aqueous solution, in crystals, in metal complexes or on lipid membranes.

Abbreviations: IRATR, infrared attenuated total reflection (spectroscopy); POPC, 1-palmitoyl-2-oleoyl-*sn*-glycero-3-phosphocholine.

Present addresses: Chemistry Department, University of Athens, Athens, Greece (P. M.); Division of Material Chemistry, Kyoto University, Yoshida Honmachi, Sakyo-ku, KYOTO, Japan 606-01 (S. K.); Sandoz Ltd, Basel, Switzerland (H.-U. G.)
Address for correspondence: Dr R. Schwyzer, Prof. emerit. ETH, Hartriegelstrasse 12, CH-8180 Bülach, Switzerland.

CCC 1075-2617/97/010065-17

In aqueous solution, however, conformational equilibria rather than single, preferred conformations of enkephalins are found [7]. In crystals, X-ray diffraction revealed a high degree of conformational polymorphism, with extended, single-bend or double-bend secondary structures [8].

This makes it impossible to define solution or crystal structures of the endogenous enkephalins as receptor-preferring conformers. Conformation analysis of cyclic receptor-selective analogues appears to be a more promising approach, although equilibria among different conformers of the cyclic molecules are still possible [9]. Constrained analogues with δ- or μ-selectivity have been obtained through backbone and side-chain cyclization (e.g. [5, 10]), or through complexation with Ca^{2+} [11]. However, those conformational features specifically determining μ- or δ-receptor preference remain elusive.

Preferred conformations of opioid peptides on artificial lipid membranes are interesting, because accumulation, conformation and orientation of opioid peptides in different membrane compartments were found to correlate with δ-, μ- and κ-receptor potency and selectivity [12–14].

Thus, a lipid-induced α-helix comprising the nine N-terminal residues was detected for dynophin A-(1–13) with infrared attenuated total refection (IRATR) spectroscopy [15] and for dynorphin A-(1–17) with ^{1}H 2D NMR [16]. The induced helical domain and its specific location and orientation on artificial lipid membranes appears to augment κ-receptor selectivity of opioid peptides [12, 17] (for applications of the concept, see [18, 19]).

The study of weakly adsorbed peptides, such as the enkephalins [20–24], is quite difficult because of the low surface density of adsorbed molecules at saturation. Nevertheless, the group of the late Tatsuo Miyazawa, using ^{1}H TRNOE NMR [25], found a folded structure of the synthetic analogue, [D-Ala^2, Leu^5]-enkephalin, on micelles prepared from mixtures of perdeuterated phosphatidyl choline and phosphatidyl serine. This μ-selective agonist contains a γ- and a $\beta_{II'}$-turn, distinguishing it from the inactive diastereomer, [D-Ala^2, Leu^5]-enkephalin. The authors suggest that membrane-induced orientations of such conformers which expose the Tyr^1 residue toward the aqueous phase may be important for μ-agonist activity. A novel β_{IV}-turn conformer of [Leu^2]-enkephalin on perdeuterated dodecyl phosphocholine micelles was detected by NMR spectroscopy by the group of Kallick [26].

IRATR spectra obtained in 1983 with [L-Tyr^1, L-Phe^4, L-Leu^5]-enkephalin and [D-Tyr^1, D-Phe^4, D-Leu^5]-enkephalin on neutral lipid multibilayers prepared from 1-palmitoyl-2-oleoyl-*sn*-glycero-3-phosphocholine (POPC) indicated like preferred conformations and orientations of the two peptides (unpublished laboratory reports by H.-U. Gremlich, S. Kimura and P. Minakakis). In the meantime IR characteristics of peptide turns were extensively reviewed [27, 28], and β_{III}-turns, α-turns and γ-turns emerged as possible membrane structures of the two enantiomeric enkephalins [13; p. 336–367].

In this paper, we describe our 1983 experiments and present a recent interpretation of the spectra based on a second derivative analysis, suggesting (non-zwitterionic) 3_{10}- and α-helix structures along with, possibly, β_I- and γ_I-turns. PCMODEL dynamics and minimization procedures indicated robust (non-zwitterionic) 3_{10}-helices and fragile α-helix structures that convert to double-bends with backbone dihedrals of the well-known Aubry β_{III}/β_I turn crystal conformation [29]. The SYBYL standard procedure, however, changed both the 3_{10}-helices and the Aubry β_{III}/β_I turn crystal conformation α-helices. Modelling of zwitterionic 3_{10}-helical [Leu^5]-enkephalin with PCMODEL produced a double-bend secondary structure containing a type C_{13} turn (distorted α-turn) bridged by a γ_I-turn with close interaction between the charged C- and N-termini. This was reminiscent of the Miyazawa (γ_I, $\beta_{II'}$)-turn structure of [D-Ala^2, Leu^5]-enkephalin. In the modelled helical and Aubry structures, the orientations of the amide I and II transitions moments were able to produce the measured dichroic ratios, but in the zwitterionic structures, they were not.

MATERIALS AND METHODS

Chemicals

1-Palmitoyl-2-oleoyl-*sn*-glycero-3-phosphocholine (POPC) was purchased from R. Berchtold, CH-3007 Bern. [L-Leu]-enkephalin and [L-Leu]-enkephalinamide, HCl, were from Bachem (CH-4416 Bubendorf).

[D-Tyr^1, D-Phe^4, D-Leu^5]-enkephalin (**8**) was synthesized in solution according to Scheme 1, where DCC is dicyclohexylcarbodiimide and HOBT is 5-hydroxybenzotriazole. Intermediates and products were purified and characterized by crystallization (where possible), thin layer chromatography on Merck precoated silica gel plates in five different solvents, optical rotation and elemental analysis, the latter two in the analytical laboratories of the Organic Chemistry Dept., ETH Zürich.

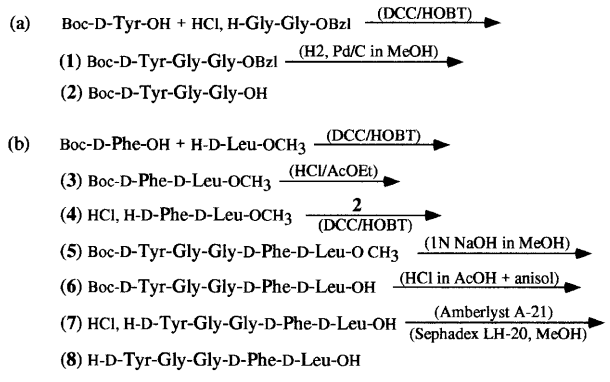

Scheme 1 Synthesis of *all*-D-[Leu^5]-enkephalin, **8**.

From moist methanol and diethylether, **8** crystalized with 1.5 molecules of water in a total yield of 23% (from **1**). R_F 0.52 (*n*-BuOH, AcOH, H_2O, 100/10/30 volume parts); R_F 0.28 (ethylacetate, puridine, formic acid water, 63/91/10/6 volume parts). Melting point: 160–161 °C. $[\alpha]_{578}^{25} = +20.6°$ ($c = 0.8$ in dimethylformamide). $C_{28}H_{40}O_{8.5}N_5$ (582.62): % found (% calc.) C 57.62 (57.72), H 6.73 (6.92), N 11.84 (12.01).

[D-Tyr^1, D-Phe^4, D-Leu^5]-enkephalinamide, HCl was synthesized in a similar manner using H-D-Leu-NH_2 in place of H-D-Leu-OCH_3 and was compared with a sample of its enantiomer, [L-Tyr^1, L-Phe^4, L-Leu^5]-enkephalinamide, HCl, with which it shared all physical properties except the sign of its specific rotation and its biological activity. It crystallized with one molecule of water from MeOH/Et_2O. R_F 0.29 (*n*-BuOH, AcOH, H_2O, 100/10/30 volume parts); R_F 0.51 (ethylacetate, pyridine, formic acid, water, 63/91/10/6). Melting point: 178–180 °C (179–180 °C for the L-enantiomer). $[\alpha]_{578}^{25} = -23.61°$ [$c = 1.08$ in dimethyformamide). The L-enantiomer (**10**) had $[\alpha]_{578}^{25} = +24.25°$ [$c = 0.94$ in dimethyformamide). $C_{28}H_{39}O_6N_6C1$ (609.13): % found (% calc.) C 55.90 (56.21), H 6.62 (6.78), N 13.69 (13.79), C1 6.22 (5.82).

[D-Tyr^1, D-Phe^4, D-Leu^5]-enkephalin methyl ester, HC1 was obtained from **5** in analogy to the reaction **6** → **7** by treatment with 3N HCl in acetic acid/anisole followed by precipitation from methanol with diethylether.

IRATR Measurements

Procedure. The experimental setup and the relevant equations are reviewed in [13, 30]. The IR absorption spectra of the samples (under N_2 at 25 °C) were measured with a Perkin-Elmer Infrared Spectrophotometer 580 equipped with an Interdata 6/16 computer as described in [31]. The internal reflection element, a ZnSe crystal ($n_1 = 2.40$), was from Harrick Scientific Corporation (Ossining, NY). The spectra were scanned alternately with light polarized parallel (pp) or vertical (vp) to the plane of the angle of incidence ('parallel' and 'vertical' electrical field components, E_p and E_v, respectively). The absorbance, $\alpha = -\log T$, in which T is transmittance, was plotted against the IR frequency, $\tilde{\nu}$ (cm^{-1}). The values represent the means from at least four separate measurements. Polarization along the *z*-axis was expressed as the dichroic ratio, $R_z = \alpha_p/\alpha_v$, where α_p and α_v are the absorbances measured as band areas in the parallel and vertical modes, respectively. Deuterium exchange experiments were carried out by exposing the samples to an atmosphere of nitrogen saturated with D_2O for 16 h at 25 °C. The rate of ^1H–^2H exchange was estimated semiquantitavely from the reduction of the ν (N–H) absorption at 3280 cm^{-1}.

Pure peptides were deposited on the ZnSe crystal by evaporation of their methanoic solutions and dried under N_2 at 25 °C. Their spectra are the difference of the total spectra minus the spectra of the ZnSe crystal. IR absorptions of the peptides were compared with those of the pure amino acids, L-tyrosine and L-phenylalanine, to verify assignments of structural features.

Model membranes were deposited on the ZnSe crystal by evaporation of a methanoic solution of peptide and POPC (molar ratio of 1:25) and then dried under pure N_2 at 25 °C for 3 h. Membrane IR spectra were measured (i) before equilibration with water, and (ii) after equilibration with liquid water at 25 °C for 10, 15 or 20 min, with subsequent drying under pure N_2 at 50 °C for 3 h. The water treatment reduced the amount of peptide in the membrane to about 30% of its original value, i.e. to a molar ratio of peptide:lipid of about 1:80. The peptide spectra were the difference of the total spectra minus the lipid membrane spectra minus the spectra of the ZnSe crystal. Two bands, one at 970 cm^{-1} (*trans* [=C–H]wag) and the other at 1470 cm^{-1} ($\delta[CH_2]$, were chosen as reference signals to determine the amount of lipid to be subtracted from the spectra. Membranes with or without peptide were composed of about four to six bilayers as judged from their interference colour [32]. On equilibration and drying, a band at 910 cm^{-1} appeared, characteristic of a choline *gauche* conformation in the liquid crystalline ultrastructure [33].

Resolution of IR Band Shapes into Component* Lorentzian Bands.** Analysis and display of the curves was performed using the program Mathcad 3.1 (MathSoft Inc., Cambridge, MA) to calculate the second derivatives and to solve the ***Lorentz equations:

$$\alpha(\tilde{\nu}) = (w/\pi) \cdot \frac{\alpha_0}{[(\tilde{\nu} - \tilde{\nu}_0)^2 + w^2]} \qquad (1)$$

Band half-widths were $w = 6.1$ and $3.25\ \mathrm{cm}^{-1}$ in the pp and vp mode, respectively. The *Lorentzian* band parameters were chosen by visual observation and comparison with the second derivatives of the reconstituted and the experimental absorption bands.

Estimation of Peptide Orientation. The dichroic ratio, R_z, is an estimate of peptide orientation relative to the coordinates of the internal reflection element. A correlation between R_z, the direction of the amide I and II transition dipole moments, and the orientation of secondary structures is established by using the model of Figure 1. Peptide and lipid molecules are subject to thermal disordering. Time-average orientation is quantified in terms of an order parameter:

$$S = \tfrac{3}{2}\langle \cos^2 \gamma \rangle - \tfrac{1}{2} \qquad (2)$$

where $\langle \cos^2 \gamma \rangle$ implies a time-average distribution of the angle γ. For a liquid crystalline ultrastructure, the z-axis as the space-fixed direction, an order parameter S, and an angle θ, the dichroic ratio is:

$$R_z = \frac{\alpha_p}{\alpha_v} = \frac{\alpha_x + \alpha_z}{\alpha_y} = \frac{E_x^2}{E_y^2} + \frac{E_z^2}{E_y^2} \cdot \frac{S(\cos^2 \theta - \frac{1}{3}) + \frac{1}{3}}{S(\frac{1}{2}\cos^2 \theta - \frac{1}{3}) + \frac{1}{3}} \qquad (3)$$

E_x, E_y and E_z are the electrical field components in x, y *and* z, respectively. They are estimated from the refractive indices of the internal reflection element (here, ZnSe, $n_1 = 2.40$), the sample (lipid, $n_2 \approx 1.55$), the surrounding media (air, $n_3 \approx 1.00$), and the incident angle (45°) [32].

Estimation of Dichroic Ratios from Molecular Models. According to Eq. (3), the dichroic rations to be expected for a given peptide conformer are a function of the alignment of the amide I transition moments (angles θ_1) and the order parameters (***S***). Ball & Stick *moldat* files were modified to include the directions of the amide I transition moments relative to the molecular axis of a given model. The direction of the molecular axis (M) in the molecular was chosen to minimize the mean deviation of the four amide I transition moments, $\theta_{1,i}$, from M.

Molecular Modelling and Dynamics Simulation

Simulation with PCMODEL. Molecular modelling and dynamics simulations were carried out on a Macintosh Centris 650 computer, equipped with a floating point unit, 24 Mbyte RAM, and operated with 80 Mbyte virtual memory. The program was provided by the molecular modelling software package PCMODEL of Serena Software (Bloomington, IN).

The force field used in PCMODEL is called MMX and is derived from the MM2(QCPE-395, 1977) force field, with the pi-VESCF routines taken from MMP1(QCPE-318), both by N. L. Allinger, and modified for open shell species, and the heat of formation calculations improved. The calculations included electrostatic interactions between atomic charges in a medium of dielectric constant 1.5.

Molecular models: Unconstrained, non-zwitterionic models of [Leu^5]-enkephalin with 3_{10}-helical (**B1** to **B3**) and α-helical (**A1** to **A3**) structures were constructed. The ψ, ϕ and χ dihedrals of Tyr^1 and Leu^5 were arbitrarily chosen near the energy minima indicated by the ROT-E subroutine of PCMODEL. The ψ/ϕ dihedrals of Gly^2, Gly^3 and Phe^4 were adjusted to the three sets of classical values described in the reviews by Dickerson & Geis [34] and Benedetti [35], thus **B1**(− 49/ − 26), **B2**(− 60/ − 30), **B3**(− 74/ − 4), **A1**(− 48/ − 57), **A2**(− 55/ − 45) and **A3**(− 67/ − 44). Screw-sense diastereomers of **B2** were constructed with the positive values of all dihedrals; their enantiomers were obtained from [D-Tyr^1, D-Phe^4, D-Leu^5]-enkephalin, i.e. **B2**(L, P), **B2** (L, M), **B2**(D, M), **B2** (D, M), where *P* (plus) and M (minus) are the screw sense descriptors. **AUB**, the crystal molecular conformer of [Leu^5]-enkephalin, was built with the backbone and side-chain dihedrals of Aubry *et al.* [29]. **B1z** was the zwitterion of **B1**(− 49/ − 26) with terminal $-COO^-$ and NH_3^+ groups. The Miyazawa membrane-bound structure of [D-Ala^2, Leu^5]-enkephalin [25] was built as a zwitterion with the x, y, z-coordinates kindly provided by Dr A. Milon (LPTF-CNRS, Toulouse); it was converted to the corresponding [Leu^5]-enkephalin zwitterion model, **MMz**, by removal of the methyl group.

Simulations were usually carried out by 'quenching', the repetition of a molecular dynamics pulse followed by energy minimization. Molecular dy-

namics were performed with equal bath and sample temperatures 400–600 °K, time steps of 1 fs, temperature relaxation times of 1 fs, viscosity of the surrounding media of 0 cp, and a total time $\approx$ 100 fs, which increased the model MMx - energies to $\approx$100 to 300 kcal/mol. The cycle was repeated five to ten times, until the energies after minimization levelled out.

The zwitterionic form of **B1**(−49/−26), was modelled with (i) minimization, (ii) 7.2 ps of molecular dynamics at 320 °K and 100 cp viscosity of the surrounding media (mimicking the lipid membrane), (iii) proton transfer from $-NH_3^+$ to $-COO^-$ to give **B1zn**, (iv) minimization, and (v) 3.6 ps of molecular dynamics. **MMz** was modelled with (i) minimization, (ii) 5 ps of molecular dynamics at 320 °K and 50 cp viscosity of the surrounding media, (iii) proton transfer from $-NH_3^+$ to $-COO^-$ to give **B1zn**, (iv) minimization, (v) rotation of the Tyr ψ angle to 2°, and (vi) molecular dynamics as above for 1.5 ps.

Simulations with SYBYL. The SYBYL molecular modelling program (Tripos Associates, St Louis, MO) is based on the MM2 force field and was run on an Indigo workstation with a Silicon Graphics terminal (courtesy of P. W. Schiller and B. C. Wilkes, Clinical Research Institute of Montreal, Canada). We used it to minimize energies and check against the results we had obtained with PCMODEL. The models used for SYBYL minimization were B1, A1 and AUB. Program-inherent 'side-chain' clean up was used for B1 and A1.

Graphics. The PCMODEL and SYBYL files were transferred to the graphics program Ball & Stick of Norbert Müller (Cherwell Scientific Publishing Ltd, Oxford OX4 4GA, UK), and from there to the graphics program Canvas (Deneba Software, Miami, FL), with which the Figures were produced.

RESULTS

IRATR Studies of *all*-L and *all*-D [Leu^5]-enkephalins

[L-Tyr^1, L-Phe^4, Leu^5]-enkephalin, [D-Tyr^1, D-Phe^4, D-Leu^5]-enkephalin and [D-Tyr^1, D-Phe^4, D-Leu^5]-enkephalin Methyl Ester Without Lipid. The spectra of the two unesterified peptides on the ZnSe crystal were identical. It was possible to assign all absorptions to chemical group vibrations (Table 1). The assignment of aromatic features was aided by comparison with tyrosine and phenylalanine. The zwitterion nature of the two 'free' peptides was clearly indicated, particularly by the symmetrical stretching vibration of the carboxylate group

Table 1 Typical IR Bands of *all*-L and *all*-D [Leu^5]-enkephalin, and of *all*-D [Leu^5]-enkephalin Methyl Ester in the Solid State

Tentative assignment	*all*-L	*all*-D	*all*-D -OMe
	(cm^{-1})	(cm^{-1})	(cm^{-1})
$\nu_{as}(NH_3^+)$	3200–2800	3200–2800	missing
ν(NH) + ν(OH) Tyr	3295	3295	3295
ν(C=O)	missing[a]	missing[a]	1740[a]
Amide I	1654/1652	1653/1651	1653/1651
ν(C=C) Tyr, Phe	1615	1614	1612
$\nu_{as}(COO^-)/\delta_{as}(NH_3^+)$	1600	1600	missing
Amide II	1540/1532	1540/1532	1540/1535
ν(C=C) Tyr, Phe + $\delta_s(NH_3^+)$	1515	1515	1515 narrowed
$\delta(CH_2)$	1468	1468	1468
ν(C=C) Tyr, Phe	1452	1452	1452
$\nu_s(COO^-)$	1402	1402	missing
δ_{ip}(OH) Tyr	1368	1368	1368
Amide III + $\nu(C_{ar}$-O) Tyr	1245	1245	1245
δ_{ip}(OH) Tyr	1172	1172	1172
$\delta_{ip}(C_{ar}$-H) Tyr, Phe	1027	1027	1025
Amide V + δ(C–C) Tyr	745/700	745/700	

[a]On the dry POPC membrane (1470 cm^{-1} as reference band) a clear absorption is seen in 1720–1730 cm^{-1}; on liquid crystal membranes, it appears as a pronounced shoulder in the same location (970 cm^{-1} as reference band). This indicates a ν(C=O) vibration in a non-zwitterionic peptide.

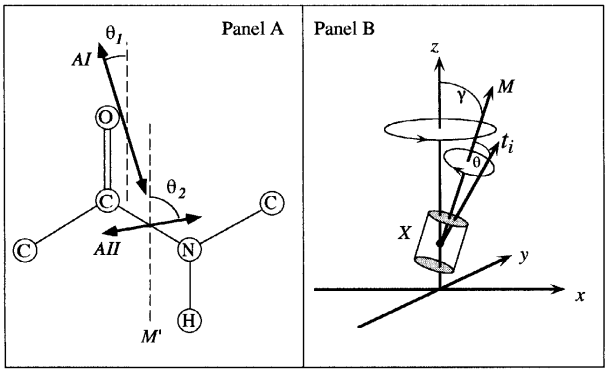

Figure 1 Estimation of peptide orientation on the IRATR internal reflection element (IRE). *Panel A*: IR transition moments of the peptide group (↔): A_I, amide I, A_{II}, amide II. θ_1 and θ_2 are the angles between the transition moment vectors and the direction of the molecular axis, *M'* (here, for illustration, *M'* is arbitrarily defied as being parallel to the carbonyl direction). For the amide I vibration, $\nu_{CO} \approx 80\%$; $\nu_{co} \approx 10\%$, $\delta_{NH} \approx 10\%$, $\theta_1 \approx 17°$, all in the plane of the peptide bond. For the amide II vibration, $\nu_{CN} \approx 40\%$, $\delta_{NH} \approx 60\%$, $\theta_2 \approx 80°$, all in the plane of the peptide bond. *Panel B*: Model of dynamic peptide orientation in liquid crystalline lipid bilayers: The coordinate system corresponds to the IRE with *z* as the space-fixed axis parallel to the angle of IR beam incidence and the bilayers spread in the *x*, γ-plane (vertical to the angle of incidence). The molecular segment, *X* with its amide I transition moments, t_i, at angles θ_i, rotates around the molecular axis, *M*, which, in turn, rotates around *z* with a narrow distribution of γ.

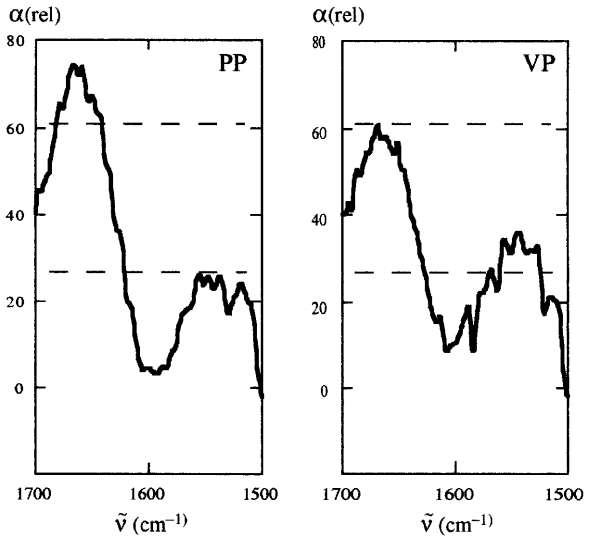

Figure 2 Polarized IRATR spectra of [Leu^5]-enkephalin on equilibrated POPC multi-bilayers (molar ratio lipid/peptide $\approx 80:1$). The IR electric field component is polarized parallel (pp) or vertical (vp) to the angle of IR beam incidence.

[ν_s(COO-)] at 1402 cm^{-1}, which was missing in the spectra of the methyl ester. The difference between the zwitterion and neutral molecules also shows in the 1740 cm^{-1} region, where the [ν(C=O)] absorption is present in the methyl ester but is missing in the 'free' peptides. The shape and position of the amide I band in the 1650–1655 cm^{-1} region and of the amide III band in the 1240–1330 cm^{-1} region suggested the presence of β-turn conformations [27]. The polarization of the *all*-L amide I band was measured as $R_z = 1.23 \pm 0.06$, that of the *all*-L amide II band as $R_z = 1.0 \pm 0.1$, indicating an orientation of the amide I and II transition dipole moments perpendicular and parallel to the carrier surface, respectively. In the solid peptides, about $91 \pm 2\%$ of all amide protons were readily exchanged for deuterons in an atmosphere of nitrogen saturated with D_2O.

Peptide–lipid mixtures of all-L and *all*-D-[Leu^5]-enkephalin with 1-palmitoyl-2-oleoyl-*sn*-glycero-3-phosphocholine (POPC). In *non-equilibrated, gel state membranes*, the amide I and II bands of both peptides revealed maxima in the 1665–1670 and 1500–1550 cm^{-1} regions, respectively. The dichroic ratios indicated a principal orientation of both the amide I and II oscillators along the *z*-axis, perpendicular to the membrane surface (Table 2).

In the *equilibrated, liquid crystalline membranes*, the amide I and II maxima of both peptides again appeared between 1665–1670 and 1500–1550 cm^{-1} respectively. Their dichroic ratios were distinctively different from those in the solid state and in the non-equilibrated membranes (Table 2), indicating a strong orientation of the amide I oscillators along the *z*-axis and the amide II oscillators in the *x*, *y*-plane. In an atmosphere of nitrogen saturated with D_2O (16 h, 25 °C), only about 10% of the peptide amide protons were readily exchanged for deuterons.

Interpretation of the Spectra in Terms of Peptide Conformation and Orientation

The interpretation took into account both the *Lorentzian* amide I band pattern and the polarization of the amide I and II bands. The *Lorentzian* analysis suggested reverse turns, the exact identification of which was only partly possible, because 'frequencies are very dependent on the particular dihedral angles of the turn' (quoted from [27], p. 301). The polariza-

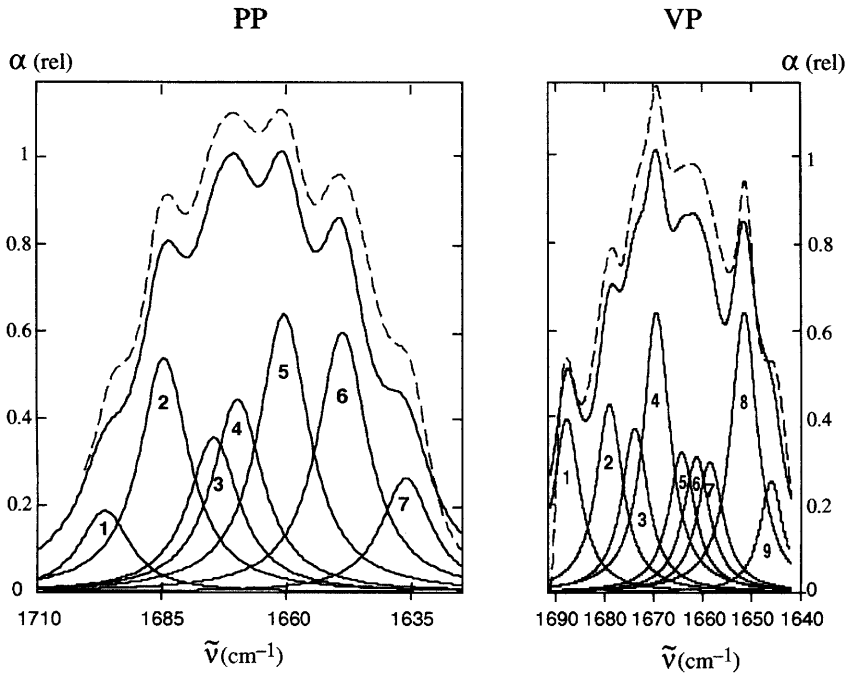

Figure 3 *Lorentz* analysis of the peptide amide I bands of [Leu^5]-enkephalin on POPC membranes. The *Lorentz* bands are numbered; their sum is the continuous curve; the broken line curve (displaced to higher relative absorbance) represents the experimental spectra.

tion indicated a global orientation of the amide I transition moments perpendicular to the membrane surface and of the amide II oscillators parallel to the membrane surface. In most reverse turns, however, the different orientation of the individual amide I oscillators within the molecules would preclude their global orientation in a preferred direction within a molecular ensemble. A sequence of two β_{III}-turns, see [36], or an α-turn would exhibit the required orientation (as observed for α-helices [15, 31, 37, 38]).

Amide I Band Patterns. A *Lorentzian* analysis of the amide I bands obtained with parallel and vertical polarized radiation is shown in Figure 3. The results are by no means thought to be the best and only ones possible. But they yielded a plausible interpretation of the IR data in terms of conformational models which were used as starting points for computer simulations. The amide II band was not considered to be of sufficient diagnostic value and was not analysed.

Figure 4 compares the results of our *Lorentzian* analysis (panel **A**) with calculated and observed band positions taken from the literature. The comparison reveals a possible presence of β_{III}-turns, short 3_{10}-helices, and α-helix building units in membrane-bound enkephalin. Frequencies and ranges estimated or observed for β_{III}-turns [27, 28, 39], and shown in panels **B** and **C**, correspond to the Lorentzian frequencies marked with *** and **.

Furthermore, the presence of α-turns is indicated by the bands marked x, corresponding to the options offered in panel **D** [28]. The strong band at 1669 cm^{-1} may represent either β_I and γ-turns (panel **B**) or short sections of 3_{10}-helix (panel **C**), whereas the 1679 cm^{-1} band falls in the range for β_{III} & C=O absorptions of panel **B**.

Amide I Oscillator Orientation (Table 2). For enkephalin in *unequilibrated membranes*, the dichroic ratios derived from the amide I and II bands were significantly greater than the isometric value of 1.00. The estimated order parameters for amide I transition moments parallel to the molecular axis ($\theta_1 = O^0$) and amide II oscillators at $\theta_2 = 80°$ were estimated as $S_1 = 0.45$ (amide I) and $S_2 = -0.80$, the latter well outside the allowed negative limit of -0.5. Assuming $\theta_2 = O°$, then $S_2 = 0.36$, indicating principal orientations of both the amide I and II oscillators parallel to the z-axis.

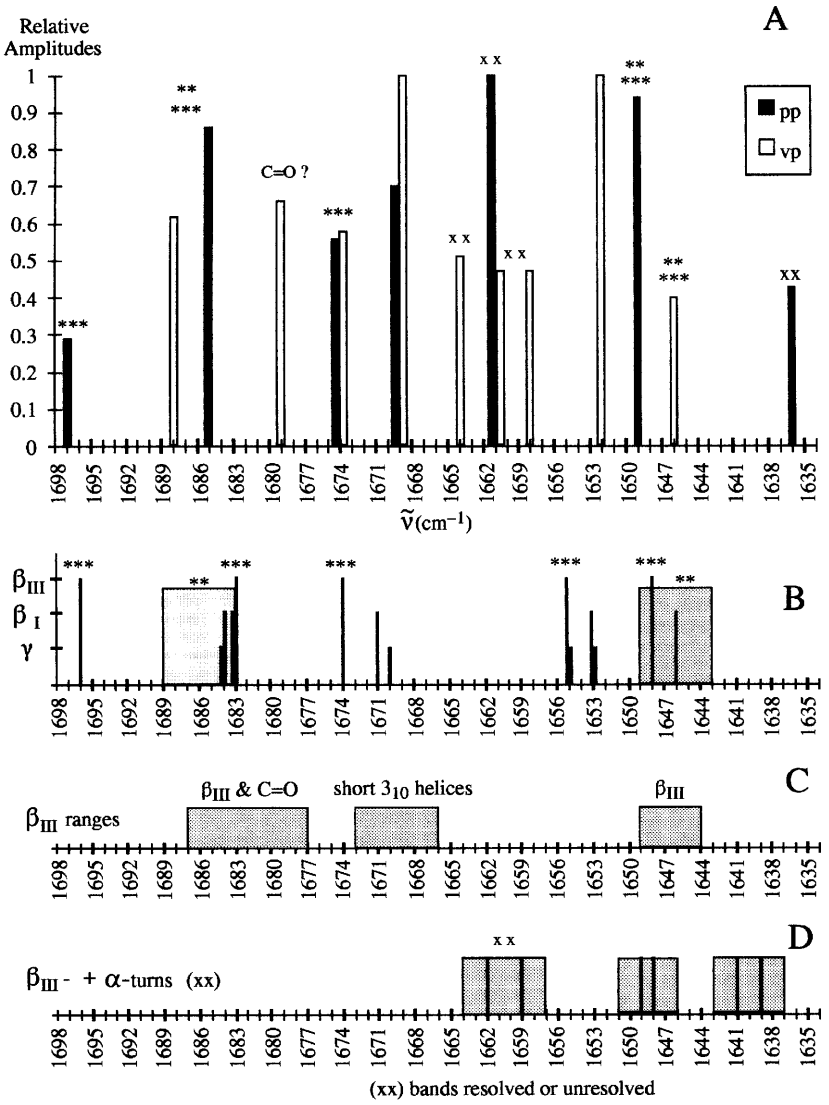

Figure 4 Interpretation of the Lorentz analysis in terms of secondary structure. Panel **A**: positions and relative amplitudes of the Lorentz bands of Figure 3. Panel **B**: frequencies estimated from insulin crystallographic data for β_I-, β_{III}- (***) and γ-turns [27] and the ranges observed in Krimm's group for β_{III}-turns (***)[39] (the three types of turn are distinguished by the length of the frequency indicator). Panel **C**: frequency ranges of β_{III}-turn and 3_{10}-helix absorptions. Panel **D**: absorption ranges of β_{III} turns of short 3_{10}-helices (in combination with α-turns: xx) [28].

For equilibrated, liquid crystalline membranes, the dichroic ratios and order parameters of Table 2 were quite similar for the two lipid estimates derived from either 970 or the 1470 cm^{-1} absorption. Only after washing for 20 min was the correspondence poor. This was probably caused by too strong a reduction of the amount of peptide remaining on the membrane to allow absorbance measurements of adequate precision. The estimated order parameters indicate a principal orientation of the amide I oscillators along the space-fixed *z*-axis and of the amide II oscillators in the *x*, *y*-plane.

Molecular Modelling of Possible Membrane-induced [Leu^5]-enkephalin Conformations.

The results are shown in Tables 3 and 4 and Figures 5–8.

The 3_{10}-helix. Under the simulation conditions with PCMODEL, the 3_{10}-helical structures **B1, B2**

Table 2 Dichroic Ratios, R_z, for Different DOPC/[Leu^5]-enkephalin Mixtures in the Amide I and Amide II Infrared Absorption Ranges. The Model Membranes are either in Their Gel State (no H_2O)[a] or Their Liquid Crystalline State (liq. H_2O)[b]. The Order Parameter, S_z, Was Estimated Assuming a Principal Orientation of Each Type of Oscillator (Amide I and II) Perpendicular to the Membrane Surface ($\theta_1 = \theta_2 = 0°$).

Peptide	IR Band	*DIchroic ratios*, R_z [c]		S_z	Membrane
		ref. 1470cm $^{-1}$	ref. 970 cm^{-1}	$\Theta_1 = \Theta_2 = O°$.	
all-D	Amide I	1.50	1.50	0.45[d]	no H_2O liq.
all-D	Amide II	1.36	1.35	0.36[d]	no H_2O liq.
all-L	Amide I	1.50 ± 0.10	–	0.45[d]	liq. H_2O 15 min
all-L	Amide II	0.9 ± 0.1	–	− 0.18[d]	liq. H_2O 15 min
all-D	Amide I	1.36	1.33	0.35[d]	liq. H_2O 10 min
all-D	Amide II	0.83	0.85	− 0.33[d]	liq. H_2O 10 min
all-D	Amide I	1.26	1.38	0.38[e]	liq. H_2O 20 min
all-D	Amide II	0.59	0.85	− 0.30[e]	liq. H_2O 20 min

[a]Molar ratio lipid/peptide = 25.
[b]Molar ratio lipid/peptide $\approx$ 80.
[c]R_z values determined with bands at 1470 and 970 cm^{-1} as reference values for lipid absorbance.
[d]From the average of the R_z values determined with ref. 1470 and 970 cm^{-1}.
[e]From the R_z value determined with ref. 970 cm^{-1}.

and **B3** proved to be very robust. After disruption during the dynamics step, the H-bond pattern of two β_{III}-turns reappeared without metastable, otherwise folded intermediates. The simulation end products were the models **B1** (–13.82), **B2** (–12.62), and **B3** (–11.96), where the numbers in parentheses indicate MMX energies in kcal/mol. The internal alignment of the amide I transition moments of all three predicts the observed experimental dichroic ratios within plausible limits of order parameters and orientations of the molecular axes.

With the SYBYL energy minimization program, the 3_{10}-helical structure **B1** (–49/–26) was converted to an α-helix with a SYBYL energy of –6.24 kcal/mol (SYBYL and MMX energies cannot be compared).

The α-helix and the Aubry Crystal Molecular Conformation. With the same PCMODEL 'quenching' protocol, the α-helical structures of [Leu^5]-enkephalin proved to be less robust than the 3_{10}-helices, since, in the minimization step after molecular dynamics, metastable intermediates with different H bond patterns appeared before the energy minima were reached.

A1 (–48/–57) produced the 13-membered H-bonded cyclic (C_{13}) α-turn **A1** (–11.66) after a number of intermediate stages: first, a structure with a ($\beta_{III} + \beta_I$) double bend, which resembled that of the Aubry crystal conformer [29], then, a structure with a single β_{III}-bend (C_{10}) between Tyr^{1}C=O and HNPhe^4.

A2 (–55/–45) was converted to **A2** (–12.13) with a stable ($\beta_{III} + \beta_I$)-double bend ($2 \times C_{10}$), closely resembling that of the Aubry crystal conformer, after having passed through an intermediate stage with a single β_{III}-turn between Tyr^{1}C=O and HNPhe^4.

A3 (–67/–44) was converted to **A3** (–12.06), an ($\alpha + \beta_{III}$)-type (C_{13}/C_{10}) double turn structure with H-bonds between the carbonyl oxygen of Tyr^1 and the amide hydrogens of Phe^4 and Leu^5. Intermediate was a single β_{III}-turn structure with only the (Tyr^{1}C=O...HNPhe^4) H-bond.

AUB, the Aubry double bend crystal conformer experienced a slight relaxation of the (Gly^2 C=O...HNLeu) H-bond from $\approx$2.1 to $\approx$2.54 Å in the β_I-turn, and an oscillation between states of higher and lower energy, e.g. **AUB** (–12.11), **AUB** (-6.38), **AUB** (–12.42), **AUB** (–5.94) in the third to sixth cycles of the quenching procedure. **AUB** (–12.42) and **AUB** (–12.13), both meet the requirements of the observed dichroic ratios.

With the SYBYL program, the Aubry ($\beta_{III} + \beta_I$) double bend structure of **AUB**, as well as the α-turn of **A1**, were converted to identical α-helices with SYBYL energies –6.237 kcal/mol. This preference of an α-turn may be caused by the fact that the SYBYL force field – as used here – is primarily designed to meet the needs of protein and large peptide modelling, whereas the PCMODEL force field is designed to

Table 3 Dihedral Angles and MMX Energies of Simulated [Leu^5]-enkephalin Conformers. The Leu^5 ψ_i Angle was Measured to the Carboxylate OH Group; for Aromatic Side Chains only the $\chi^2_{i,1}$ Angles are Shown, Assuming the $\chi^2_{i,1}$ Angles to Differ by $\approx 180^\circ$

	Dihedrals					
Residue/Model	ϕ_i	ψ_i	w_i	χ^1_i	$\chi^2_{i,1}$	$\chi^2_{i,2}$
Tyr^1 B1(−13.82)	–	130.18	179.70	178.10	65.72	
B2(−12.62)	–	83.50	179.30	178.25	65.47	
B3(−11.96)	–	33.88	179.12	−55.72	109.62	
A1(−11.66)	–	113.16	173.12	170.64	60.00	
A2(−12.13)	–	90.26	177.50	179.78	69.41	
A3(−12.06)	–	20.88	173.49	−54.65	104.14	
AUB(−12.42)	–	117.48	175.64	179.43	64.2	
B1zn(−8.54)	–	145.66	−175.03	−178.45	69.41	
MMzn(−10.14)	–	29.76	−179.36	−57.22	107.97	
Gly^2 B1(−13.82)	−54.22	−25.42	178.42			
B2(−12.62)	−56.18	−19.93	178.08			
B3(−11.96)	−51.35	−28.90	177.75			
A1(−11.66)	−50.04	−39.93	−178.58			
A2(−12.13)	−55.55	−17.96	−176.90			
A3(−12.06)	−48.54	−46.33	178.30			
AUB(−12.42)	−51.12	−31.16	176.46			
B1zn(−8.54)	−56.42	−54.15	177.75			
MMzn(−10.14)	−82.46	+58.22	−178.88			
Gly^3 B1(−13.82)	−65.75	−3.09	170.79			
B2(−12.62)	−63.72	−10.47	172.56			
B3(−11.96)	−61.82	−11.20	175.02			
A1(−11.66)	−58.87	−41.60	−174.60			
A2(−12.13)	−61.56	−30.92	−175.53			
A3(−12.06)	−63.09	−30.36	176.21			
AUB(−12.42)	−60.54	−39.57	177.32			
B1zn(−8.54)	−81.11	58.73	−174.54			
MMzn(−10.14)	+65.64	−95.02	179.34			
Phe^4 B1(−13.82)	−79.52	−24.18	−172.57	178.17	67.44	
B2−12.62)	−76.30	−19.97	−171.90	177.74	72.48	
B3(−11.96)	−77.69	−19.36	173.45	−177.85	72.68	
A1(−11.66)	−85.73	−22.10	176.83	−179.68	73.13	
A2(−12.13)	−85.99	−2.39	−172.14	−179.17	−74.17	
A3(−12.06)	−89.15	−14.32	−173.07	−177.23	72.70	
AUB(−12.42)	−89.75	+2.18	176.57	−51.78	148.26	
B1zn(−8.54)	176.76	−32.03	−175.23	177.12	71.72	
MMzn(−10.14)	−71.82	−24.78	179.63	−53.69	99.15	
Leu^5 B1(−13.82)	−54.13	42.28	–	−62.41	69.68	−57.04
B2(−12.62)	52.91	42.27	–	−64.30	67.98	−58.43
B3(−11.96)	54.67	41.18	–	−69.17	68.05	−169.72
A1(−11.66)	52.20	44.82	–	−158.59	71.01	−166.96
A2(−12.13)	55.60	36.47	–	−62.88	64.39	−62.44
A3(−12.06)	54.29	38.74	–	−60.42	80.01	−158.26
AUB(−12.42)	−154.95	72.72	–	−157.73	174.60	−62.28
B1zn(−8.54)	59.84	62.56	–	−53.89	170.81	−66.77
MMzn(−10.14)	−90.09	75.43	–	−65.71	79.50	−158.78

Table 4 Estimated Orientation Parameters (Figure 1) of the Local Minima Conformers of [Leu^5]-enkephalin.

Model	θ°	R_z	S	γ°
B1(−13.82)	**21.4**	1.37	0.46	36.87
B2(−12.62)	**16.81**	1.37	0.42	38.29
B3(−11.96)	**15.12**	1.37	0.41	38.84
A1(−11.66)	**14.30**	1.37	0.41	38.84
A2(−12.13)	**22.16**	1.37	0.47	36.47
A3(−12.06)	**18.61**	1.37	0.44	37.66
AUB(−12.42)	**24.10**	1.37	0.49	35.51
B1zn(−8.54)	**32.98**	1.37	0.67	27.97
MMzn(−10.14)	**63.22**	1.00	0.00	54.74
β_{IV}-turn	**72.04**	1.00	0.00	54.74

R_z = Dichroic ratio observed for the [Leu^5]-enkephalin amide I absorption; S = Order parameter necessary to achieve R_z with θ_1 estimated from the models (e.g. Figure 6). The model signatures are those of Table 3. The β_{IV}-turn is the model from [26].

handle organic and metallo-organic molecules of low to moderate molecular weight.

The Zwitterionic Double-bend and the Miyazawa Membrane Structure. Unconstrained molecular modelling of the zwitterionic form of **B1** (−49/−26) led to the non-zwitterionic **B1zn** (−8.54). It contains a (C_{13}) α-turn between [Leu^5]NH and O=C(Tyr^1) bridged by a (C_7) γ_I-turn between (Gly^3)NH and O=C(Gly^2).

Unconstrained modelling of **MMz** gave **MMzn** (−10.14), a structure with backbone dihedrals very close to those of [D-Ala^2, L-Leu^5]-enkephalin and a (C_7) γ_I-turn between (Tyr^1)C=O and HN(Gly^2) fused to a (C_{10}) $\beta_{II'}$-turn between (Gly^2)C=O and HN(Leu^5).

Enantiomers and Diastereomers of the 3_{10}-helix. [Leu^5]-enkephalin isomers with different configurations (*all*-L/*all*-D) and helical screw sense (*P*/*M*; right-/left-handed) were built with the appropriately signed dihedrals of **B2** and subjected to molecular modelling (PCMODEL). As expected, the enantionmer pair, **B2** L, P (−9.41) and **B2** D, M (−9.32) had the same final energy, different from that of the diastereomeric enantionmer pair, **B2** L, M (−6.5) and **B2** D, P (−5.4). The dihedrals of the enantiomer pairs were quite similar (except for the sign) to those of all other 3_{10}-helical models.

Orientation of the Amide I Transition Moments in Molecular Models: Estimated and Experimental Dichroic Ratios (Table 4 and Figure 6). All the conformers modelled from the α-turn and the 3_{10}-helix, as well as the crystal conformer of Aubry *et al.* [29], met the requirement of $R_z = 1.37$, $S \approx 0.4$. **B1zn** (−8.54), needed a high value of the order parameter ($S \approx 0.7$) to attain $R_z = 1.37$, and its contribution to the observed dichroic ratio may be marginal. **MMzn** (−10.14) and the β_{IV}-turn conformer of Watts *et al.* [26] exhibit isotropic orientation of the oscillators and would not contribute to the observed dichroic ratio. (The α-turns generated by SYBYL all exhibit the required orientation parameters.)

DISCUSSION

Experimental Observations

In this study, we used IRATR spectroscopy to find lipid-induced secondary structures and orientations of the two enantiomeric [Leu^5]-enkephalins, L-Tyr-Gly-Gly-L-Leu, and D-Tyr-Gly-Gly-D-Phe-D-Leu, on flat multi-bilayers of 1-palmitoyl-2-oleoyl-*sn*-glycero-3-phosphocholine (POPC). IRATR is a powerful tool for determining lipid structure in membranes [32, 33, 40]. It is extensively used to study preferred conformations and orientations of peptides on artificial lipid membranes [15, 31, 37, 38, 41–47]. The conformational analysis is based on IR band positions and shapes, and IR dichroism serves to estimate the orientation of IR amide I and II transition moments relative to the membrane surface (reviews [13, 30]).

The zwitterionic form of *all-L* and all-D-[Leu^5]-enkephalin is manifest in the IRATR spectra of the solid-state peptides spread on the internal reflection element; however, in contact with hydrated POPC multi-bilayers, the non-zwitterionic form predominates. Easy exchange of the amide protons by deuterons and weak polarization of the amide I and II bands in the solid state yield to low exchange rates and increased polarization of the amide I and II bands of dissolved peptides on equilibrated, liquid crystalline membranes at low peptide/lipid ratios. (In gel state membranes, however, and at higher peptide concentrations, the polarization pattern was quite different, but was not analysed.) From the observed exchange rates and polarizations, we may conclude that [Leu^5]-enkephalin is situated in a rather hydrophobic part of the aqueous-hydrophobic surface gradient [48, 49] on the liquid crystalline POPC membranes and that they are oriented with a time-average slant, $\gamma \approx 35^\circ$.

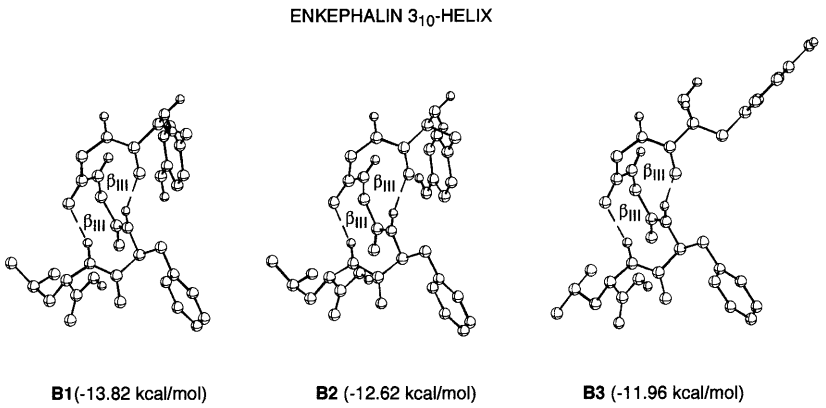

Figure 5 Molecular models of the stimulated [Leu^5]-enkephalin 3_{10}-helices (two β_{III}-turns). Dihedrals, see Table 3. Hydrogen bonds are shown as broken lines.

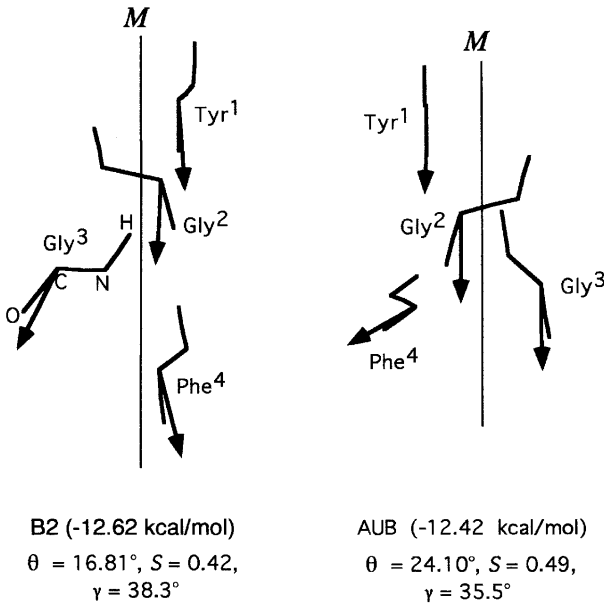

Figure 6 Alignment of amide I transition moments along the molecular axis, *M*, in [Leu^5]-enkephalin simulated models (further examples, Table 4).

Backbone Conformations

What, then, is the secondary structure of the oriented [Leu^5]-enkephalin molecules? Two points need special consideration: (i) the polarization of the amide I and II bands calls for a significant alignment of the respective oscillators in the molecules which is only possible with helical and certain double-bend secondary structures; (ii) second derivatives and *Lorentz* band analysis (see [37]) suggested 3_{10}-helices (β_{III}-turns), α-turns and, perhaps, β_I and γ-turns as ingredients of a complex mixture of secondary structures of non-zwitterionic peptides. A third point is the similarity of the spectra of the enantiomeric *all*-L and *all*-D-[Leu^5]-enkephalins on 1-palmitoyl-2-oleoyl-*sn*-glycero-3-phosphocholine (POPC) membranes which indicates loose, non-specific binding, since strong complexes with the chiral lipid are expected to be diastereomeric and to display different physical properties.

Local Minima Structures. We considered short 3_{10}- and α-helices (β_{III}- and α-turns) of *non-zwitterionic* [Leu^5]-enkephalin as candidates for our molecular modelling studies. These were designed to see whether the helical species represented local energy minima or whether they would convert to such. To achieve a certain diversity of starting models, the 3_{10}- and α-helices were constructed with the three sets of 'classical' ϕ, ψ dihedrals reported in [34, 35]. The side-chain dihedrals proved to have little influence on the outcome of the minimization and dynamics procedures. The 3_{10}-helices were quite robust, leading 3_{10}-helical end-products, **B1** (−13.82), **B2** (−12.62), and **B3** (−11.96), with rather similar energies (in parentheses, kcal/mol) and dihedrals. The α turns were less robust, converting to different types of intermediate and final products. End products were the α-turn **A1** (−11.66), the ($\beta_{III} + \beta_I$) double bend crystallographic secondary structure of Aubry *et al.* [29], **A2** (−12.13), and the combination of an α-turn with a β_{III}-turn, **A3** (−12.06). Again, the energies were quite similar and comparable to the energy of the modelled Aubry crystallographic conformer, **AUB** (−12.42). On a side-line, we note the SYBYL force field, primarily designed to meet the needs of protein and large

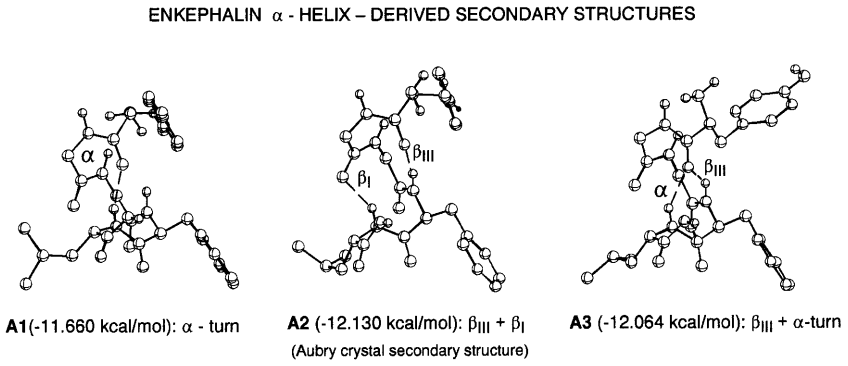

Figure 7 Molecular models that resulted from [Leu^5]-enkephalin α-helices (one α-turn) upon simulation. Dihedrals, Table 3. Hydrogen bonds are shown as broken lines.

peptide modelling, converted all the helical and the double-bend models to identical α-turns whereas the PCMODEL force field behaved in a very selective manner.

Modelling of the *zwitterionic* form of **B1** followed by proton transfer led to a non-zwitterionic model, **B1zn** (−8.54), a $C_{13}+C_7$ ('α'$+\gamma$) double bend structure. It is produced by the strong electrostatic force between the C- and N-terminal charges when modelled in a surrounding of dielectric constant 1.5 (default of PCMODEL). Whether or not the conditions for such an interaction are provided by the models membrane surface was not investigated. However, some indications of γ-turns were found in the spectra.

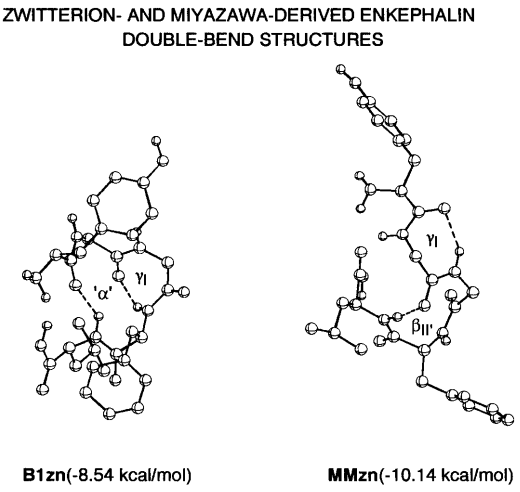

Figure 8 Zwitterion-derived [Leu^5]-enkephalin structures, Table 3. In **B1zn**(− 8.54), a 7-membered γ_I-turn ($\phi=-81°$, $\psi=59°$) is located around Gly^3 and bridges an unclassified 13-membered turn with a (Tyr^1)C=O-HN(Leu^5) bond. In **MMzn** (−10.14), the γ_I-turn is around Gly^2 ($\phi=82°$, $\psi=58°$) and is fused to a 10-membered $\beta_{II'}$-turn with a (Gly^2)C=O–HN(Leu^5) H-bond.

A Plethora of Enkephalin Membrane Structures on Membranes

Since all of the helix-derived local minima structures, 3_{10}-helix, α-turn and the double-bend structures, ($\alpha+\beta_{III}$) and ($\beta_{III}+\beta_I$), had similar MMX energies and also the necessary alignment of amide I oscillators to be able to produce the observed dichroic ratios within reasonable limits of order parameters and angles, γ, of the molecular axes, we are inclined to think that all of these secondary structures may be present [Leu^5]-enkephalin on model membranes. The diasteromeric species, L-residue/M-helix and D-residue/P-helix, were energetically unfavourable by about 3 kcal/mol and therefore less probable. This also applies to the zwitterion-derived model, **B1zn** (−8.54), which has a less favourable alignment of its amide I oscillators.

Orientation of the Molecular Axis

Whether the N- or the C-terminus points towards the aqueous compartment, was not determined experimentally. A conjecture based on the possible interaction between helix and membrane electric dipole moments [48, 50] favours an orientation in which the N-terminal tyrosine is exposed to the aqueous compartment; this view gains support by the presence of the more hydrophobic Phe and Leu side chains at the other end of the models.

NMR-derived Conformers

^{1}H-NMR transferred nuclear Overhauser effect analysis of [Leu^5]-enkephalin, [D-Ala^2, L-Leu^5]-enkephalin and [*D*-Ala^2, L-Leu^5]-enkephalinamide (agonists) and [L-Ala^2, L-Leu^5]-enkephalin (inactive analogue) bound to small unilamellar vessels (SUV) prepared from perdeuterated L-α-dipalmitoylphosphocholine (DPPC-d_{80}) and dilauroylphosphatidyl-*d*,*l*-serine (DLPS-d_{54}) in equimolar proportion suggested different backbone conformations and orientations of the biologically active and inactive species. The three active peptides, when bound to membranes, adopt the same conformation, characterized by a type II' β-turn around Gly^3-Phe^4 and a γ-turn around Gly^2 (or D-Ala^2), and their tyrosine residues are exposed on the membrane surface. The inactive compound has a completely different conformation and its tyrosine residue is inserted into the membrane [25]. It was concluded that the former orientation may be necessary for a preferred interaction with opioid μ-receptors. The authors point out that in their active conformation, 'the C-term. carboxyl group and the methyl group of Ala^2 can be connected by adding one methylene group without affecting the conformation, and then that can be the compound synthesized by Schiller and DiMaio' [51] which is μ-selective. The alignment of amide I oscillators in this ($\beta_{II'} + \gamma$) turn does not account for the dichroic ratios observed in our experiments.

Kallick *et al.* [52] point out the usefulness of micelles prepared from perdeuterated dodecylphophocholine (DPC-d_{38}) in solution NMR to determine the conformation of lipid-bound peptides (e.g. dynorphin A-(1–17) and [Leu^5]-enkephalin). Whereas the former structure was found to have an N-terminal α-helix comprising nine residues very similar to that measured by IRATR for dynorphin A-(1–13) on POPC multi-bilayers [15], the conformation of [Leu^5]-enkephalin [26] is quite different from our IRATR structures. It is described as a type IV β-turn with a close association of all side chains and no intramolecular hydrogen bond. The Phe^{4}NH is sequestered between the Leu^5 and Phe^4 side chains and the carbonyl oxygens all point away from the turn. The alignment of amide I oscillators in this β_{IV} turn cannot account for the dichroic ratios observed here.

Whereas the strongly membrane-interactive dynorphines are present in practically identical conformers on such different model membranes as flat multi-bilayers and micelles, the weakly adsorbed enkephalins show different behaviour in multi-bilayers, micelles and liposomes. This is not surprising, since these model membranes are expected to differ quite strongly in head group packing and surface pressure, which will allow insertion of one and the same peptide to different extents. For strongly interacting species, such as the dynorphins, the differences are expected not to be as important as for weakly interacting species. This may be an explanation for the different enkephalin structures discussed here, although it remains to be investigated more closely.

Biological Implications

The oriented helical structures of [Leu^5]-enkephalin resemble the micelle-bound NMR structure of deltophin [53], and the arguments presented there for its opioid δ-receptor preference could also apply to our membrane-induced conformers. The Miyazawa and the Watts conformers, on the other hand, are supposed to carry information for μ-receptor preference [25, 26]. Helices of opposite orientation are known to correlate with the selection of opioid κ-receptor [17, 48]. Comparisons with conformations of δ–selective antagonists, such as DPDPE [54] or *TIP*(P) peptides and naltrindole [55–57] appear to be too far-fetched for the moment.

Thus the relationship of lipid-induced structures of [Leu^5]-enkephalin to possible receptor-induced and receptor-selective structures remains an unsolved question. The thermodynamic advantage of lipid-induced folding and orientation for receptor selection is probably still best represented by the concept of membrane compartments [12, 17, 48], in which electrostatic and hydrophobic interactions between peptides and lipid membranes are supposed to lead to preferred accumulations, orientations and conformations near the respective receptor sites. This amounts to a catalysis of peptide–receptor interactions by (membrane) surfaces, without necessarily providing a closely receptor-fitting conformation. Weakly membrane-bound peptides, such as [Leu^5]-enkephalin, may prefer to enter the receptor active site from the aqueous phase, strongly bound peptides, such as dynorphin A-(1–13) may prefer an entrance from the hydrophobic phase, through a side entrance of the seven helix transmembrane receptor, so to speak [17]. The latter is a realistic possibility as shown in the work of Moroder *et al.* [58].

ACKNOWLEDGMENT

This contribution is dedicated to the memory of the European peptide pioneer, Theodor Wieland, 1913–1995.

REFERENCES

1. J. Hughes, T. W. Smith, H. W. Kosterlitz, L. A. Fothergill, B. A. Morgan and H. R. Morris (1975). Identification of two related pentapeptides from the brain with potent opiate agonist activity. *Nature, Lond. 258*, 57–59.
2. H. W. Kosterlitz and S. J. Paterson (1985). Types of opioid receptors: Relation to antinociception. *Phil. Trans. R. Soc. Lond. B 308*, 297–297.
3. G. A. Olson, R. D. Olson and A. J. Kastin (1995). Endogenous opiates: 1994. *Peptides 16*, 1517–1555.
4. P. W. Schiller and J. DiMaio (1982). Opiate receptor subclasses differ in their conformational requirements. *Nature 297*, 74–76.
5. V. J. Hruby (1993). Conformational and topographical considerations in the design of biologically active peptides. *Biopolymers 33*, 1073–1082.
6. P. W. Schiller in: *Handbook of Experimental Pharmacology 104/I Opioids I*, A. Herz, Ed., 681–710, Springer, Berlin, 1993.
7. P. W. Schiller (1984). Conformational analysis of enkephalin and conformation–activity relationships. *The Peptides 6*, 219–268.
8. J. R. Deschamps, C. George and J. L. Flippen-Anderson (1996). Structural studies of opioid peptides: A review of recent papers in X-ray diffraction studies. *Peptide Sci. 40*, 121–139.
9. K. D. Kopple, J. W. Bean, K. K. Bhandary, J. Briand, C. A. D'Ambrosio and C. E. Peishoff (1993). Conformational mobility in cyclic oligo peptides. *Biopolymers 33*, 1093–1099.
10. W. Brandt, C. Mrestani-Klaus, H. Schinke, K. Neubert, A. Barth, R. Schmidt, P. W. Schiller and H. D. Höltje (1995). The mu opioid receptor binding pharmacophore conformation of ornithine containing cyclic beta-casomorphin analogues and related peptides. *Quant. Struct. Act. Rel. 14*, 417–426.
11. B. S. Zhorov and V. S. Ananthanarayanan (1995). Conformational analysis of the Ca2+-bound opioid peptides: Implications for ligand–receptor interaction. *J. Biomol. Struct. Dynam. 13*, 1–13.
12. R. Schwyzer (1986). Molecular mechanism of opioid receptor selection. *Biochemistry 25*, 6335–6342.
13. R. Schwyzer (1992). Conformations and orientations of amphiliphilic peptides induced by artificial lipid membranes: Correlations with biological activity. *ChemTracts – Biochem. Molec. Biol. 3*, 347–379.
14. R. Schwyzer (1995). 100 Years lock-and-key concept: Are peptide keys shaped and guided to their recepters by the target cell membrane? *Biopolym. (Peptide Sci.) 37*, 5–16.
15. D. Erne, D. F. Sargent and R. Schwyzer (1985). Preferred conformation, orientation, and accumulation of dynophiin A-(1–13)-tridecapeptide on the surface of neutral lipid membranes. *Biochemistry 24*, 4261–4263.
16. D. A. Kallick (1993). Conformation of dynorphin A (1–17) bound to dodecylphosphocholine micelles. *J. Am. Chem. Soc. 115*, 9317–9318.
17. D. F. Sargent and R. Schwyzer (1986). Membrane lipid phase as catalyst for peptide–receptor interactions. *Proc. Natl. Acad. Sci. USA 83*, 5774–5778.
18. Y. Sasaki-Yagi, S. Kimura and Y. Imanishi (1991). Binding to opioid receptors of enkephalin derivatives taking α-helical conformation and its dimer. *Int. J. Peptide Protein Res. 38*, 378–384.
19. N. Collins and V. J. Hruby (1994). Prediction of the conformational requirements for binding to the kappa-opioid receptor and its subtypes. I. Novel alpha-helical cyclic peptides and their role in receptor selectivity. *Biopolymers 34*, 1231–1241.
20. R. Schwyzer, H.-U. Gremlich, B. Gysin and U.-P. Fringeli in *Peptides 1982 (Proceedings of the 17th European Peptide Symposium, Prague)* K. Blaha and P. Malon, Eds., 55–71, de Gruytel, Berlin, 1993.
21. B. Gysin and R. Schwyzer (1983). Head group and structure specific interactions between enkephalins and dynorphin with liposomes: Investigation by hydrophobic photolabelling. *Arch. Biochem. Biophys. 225*, 467–474.
22. B. A. Behnam and C. M. Deber (1984). Evidence for a folded conformation of methionine- and leucine-enkephalin in a membrane environment. *J. Biol. Chem. 259*, 14935–14940.
23. C. M. Deber and B. A. Behnam (1984). Role of membrane lipids in peptide hormone function: Binding of enkephalins t micelles. *Proc. Natl. Acad. Sci. USA 81*, 61–65.
24. C. M. Deber and B. A. Behnam (1985). Transfer of peptide hormones from aqueous to membrane phases. *Biopolymers 24*, 105–116.
25. A. Milon, T. Miyazawa and T. Higashijima (1990). Transferred nuclear Overhauser effect analysis of membrane-bound enkephalin analogues by ^{1}H nuclear magnetic resonance: correlation between activities and membrane-bound conformations. *Biochemistry 29*, 65–75.
26. C. R. Watts, M. R. Tessmer and D. A. Kallick (1995). Structure of Leu^5-enkephalin bound to a model membrane as determined by high-resolution NMR. *Lett. Peptide Sci. 2*, 59–70.
27. S. Krimm and J. Bandekar (1986). Vibrational spectroscopy and conformation of peptides, polypeptides, and proteins. *Adv. Protein Chem. 38*, 181–364.
28. D. F. Kennedy, M. Crisma, C. Toniolo and D. Chapman

(1991). Studies of peptides forming 3_{10}- and α-helices and β-bend ribbon structures in organic solution and in model biomembranes by Fourier transform infrared spectroscopy. *Biochemistry 30*, 6541–6548.

29. A. Aubry, N. Birlirakis, M. Sakarellos-Daitsiotis, C. Sakarellos and M. Marraud (1989). A crystal molecular conformation of leucin-enkephalin related to the morphine molecule. *Biopolymers 28*, 27–40.
30. H.-U. Gremlich in: *Ullmann's Encyclopedia of Industrial Chemistry B5*, p. 429–469, VCH Verlagsgesellschaft, Weinheim 1996.
31. H.-U. Gremlich, U.-P. Fringeli and R. Schwyzer (1983). Conformational changes of adrenocorticotropin peptides upon interaction with lipid membranes revealed by infrared attenuated total reflection spectroscopy. *Biochemistry 22*, 4257–4264.
32. U. P. Fringeli and H. H. Gunthard in: *Membrane Spectroscopy*, E. Grell, Ed., p. 270–332, Springer, Berlin 1984.
33. U. P. Fringeli (1977). The structure of lipids and proteins studies by attenuated total reflection (ATR) infrared spectroscopy. *Z. Naturforsch. 32c*, 20–45.
34. R. E. Dickerson and I. Geis. *The Structure and Action of Proteins*, Harper & Row, New York 1969.
35. E. Benedetti (1996). X-ray crystallography of peptides: The contributions of the Italian laboratories. *Biopolym. (Peptide Sci) 40*, 3–44.
36. C. Toniolo and E. Benedetti (1991). The peptide 3_{10}-helix. *Trends Biochem. Sci. 16*, 350–353.
37. D. Erne, K. Rolka and R. Schwyzer (1986). Membrane structure of substance P: III. Secondary structure of substance P in 2, 2, 2-trifluoroethanol, methanol, and on flat lipid membranes studied by infrared spectroscopy. *Helv. Chim. Acta 69* 1807–1816.
38. D. Erne, and R. Schwyzer (1987). Membrane structure of bombesin studied by infrared spectroscopy. Prediction of membrane interactions of gastrin-releasing peptide, neuromedin B, and neuromedin C. *Biochemistry 26*, 6316–6319.
39. A. M. Dwiwedi, S. Krimm and B. R. Malcolm (1984). IR frequencies of reverse turns. *Biopolymers 23*, 2025–2065.
40. U. P. Fringeli, M. Schadt, P. Rihak and H. H. Gunthard (1976). Hydrocarbon chain ordering in liquid crystals investigated by means of infrared attenuated total reflection (IR-ATR) spectroscopy. *Z. Naturforsch 31a*, 1098–1107.
41. H.-U. Gremlich, U.-P. Fringeli and R. Schwyzer (1984). Interaction of adrenocorticotropin-(11–24)-tetradecapeptide with neural lipid membranes revealed by attenuated total reflection spectroscopy. *Biochemistry 23*, 1808–1810.
42. E. Goormaghtigh, L. Vigneron, M. Knibiehler, C. Lazdunski and J.-M. Ruysschaert (1991). Secondary structure of the membrane-bound form of the pore-forming domain of colicin A. An attenuated total-reflection polarized Fourier-transform infrared spectroscopy study. *Eur. J. Biochem. 202*, 1299–1305.
43. S. Kimura, D. Erne and R. Schwyzer (1992). Interaction of glucagon with artificial lipid bililayer membranes. *Int; J. Peptide Protein Res. 39*, 431–442.
44. L. Lins, R. Brasseur, M. Rosseneu, C.-Y. Yang, D. A. Sparrow, J. T. Sparrow, A. M. Gotto Jr and R.-M. Ruysschaert (1994). Structure and orientation of Apo B-100 peptides into a lipid bilayer. *J. Protein Chem. 13*, 77–88.
45. S. A. Tatulian, L. R. Jones, L. G. Reddy, D. L. Stokes and L. K. Tamm (1995). Secondary structure and orientation of phospholamban reconstituted in supported bilayers from polarized attenuated total reflection FTIR spectroscopy. *Biochemistry 34*, 4448–4456.
46. Y. P. Zhang, R. Lewis, G. D. Henry, B. D. Sykes, R. S. Hodges and R. N. McElhaney (1995). Peptide models of helical hydrophobic transmembrane segments of membrane proteins. 1. Studies of the conformation, intrabilayer orientation, and amide hydrogen exchangeability of Ac-K2-(LA)12-K2-amide. *Biochemistry 34*, 2348–2361.
47. Y. P. Zhang, R. Lewis, R. S. Hodges and R. N. McElhaney (1995). Peptide models of helical hydrophobic transmembrane segments of membrane proteins. 2. Differential scanning calorimetric and FTIR spectroscopic studies of the interaction of Ac-K2-(LA)12-K2-amide with phosphatidylcholine bilayers. *Biochemistry 34*, 2362–2371.
48. R. Schwyzer (1986). Estimated conformation, orientation, and accumulation of dynorphin A-(1–13)-tridecapeptide on the surface of neutral lipid membranes. *Biochemistry 25*, 4281–4286.
49. S. H. White and W. C. Wimley (1994). Peptides in lipid bilayers: Structural and thermodynamic basis for partitioning and folding. *Curr. Opin. Struct. Biol. 4*, 79–86.
50. R. Schwyzer (1986). Membrane structure and biologic activity of adrenocorticotorpin (ACTH) and melanotropin (MSH) peptides. Estimation of structural parameters including the influence of the helix dipole moment. *Helv. Chim. Acta 69*, 1685–1698.
51. J. DiMaio and P. W. Schiller (1980). A cyclic enkephalin analog with high *in vitro* opiate activity. *Proc. Natl. Acad. Sci. USA 77*, 7162–7166.
52. D. A. Kallick, M. R. Tessmer, C. R. Watts and C. Y. Li (1995). The use of dodecylphosphocholine micelles in solution NMR. *J. Magn. Reson. Ser. B 109*, 60–65.
53. Y. Ohno, M. Segawa, H. Ohishi, M. Doi, K. Kitamura, T. Ishida, M. Inoue and T. Iwashita (1993). Conformation of deltorphin-II in membrane environment studied by two-dimensional NMR spectroscopy and molecular dynamics calculations. *Eur. J. Biochem. 212*, 185–191.
54. G. V. Nikiforovich, O. M. Prakash, C. A. Gehrig and V. J. Hruby (1993). Solution conformations of the peptide backbone for DPDPE and its beta-MePhe4-substituted analogues. *Int. J. Peptide Protein Res. 41*, 347–361.

55. B. C. Wilkes and P. W. Schiller (1992) Molecular dynamics simulation of opioid peptide analogues containing multiple conformational restriction. *Int. J. Peptide Protein Res. 40*, 249–254.
56. B. C. Wilkes and P. W. Schiller (1994). Theoretical conformational analysis of the opoiod delta antagonist H-Tyr-Tic-Phe-OH and the mu agonist H-Tyr-*D*-Tic-Phe-NH2. *Biopolymers 34*, 1213–1219.
57. B. C. Wilkes and P. W. Schiller (1995). Comparative analysis of various proposed models of the receptor-bound conformation of H-Tyr-Tic-Phe-OH related delta-opioid antagonist. *Biopolym. (Peptide Sci.) 37*, 391–400.
58. L. Moroder, R. Romano, W. Guba, D. F. Mierke, H. Kessler, C. Delporte, J, Winand and J. Christophe (1993). New evidence for a membrane-bound pathway in hormone receptor binding. *Biochemistry 32*, 13551–13559.